A highly tilted binding mode by a self-reactive T cell receptor results in altered engagement of peptide and MHC

Dhruv K. Sethi,[1] David A. Schubert,[1] Anne-Kathrin Anders,[1,2] Annie Heroux,[3] Daniel A. Bonsor,[4] Chantz P. Thomas,[1] Eric J. Sundberg,[4] Jason Pyrdol,[1] and Kai W. Wucherpfennig[1,2]

[1]Department of Cancer Immunology and AIDS, Dana-Farber Cancer Institute, and [2]Program in Immunology, Harvard Medical School, Boston, MA 02115
[3]Department of Biology, Brookhaven National Laboratory, Upton, NY 11973
[4]Boston Biomedical Research Institute, Watertown, MA 02472

Self-reactive T cells that escape elimination in the thymus can cause autoimmune pathology, and it is therefore important to understand the structural mechanisms of self-antigen recognition. We report the crystal structure of a T cell receptor (TCR) from a patient with relapsing-remitting multiple sclerosis that engages its self-peptide–major histocompatibility complex (pMHC) ligand in an unusual manner. The TCR is bound in a highly tilted orientation that prevents interaction of the TCR-α chain with the MHC class II β chain helix. In this structure, only a single germline-encoded TCR loop engages the MHC protein, whereas in most other TCR-pMHC structures all four germline-encoded TCR loops bind to the MHC helices. The tilted binding mode also prevents peptide contacts by the short complementarity-determining region (CDR) 3β loop, and interactions that contribute to peptide side chain specificity are focused on the CDR3α loop. This structure is the first example in which only a single germline-encoded TCR loop contacts the MHC helices. Furthermore, the reduced interaction surface with the peptide may facilitate TCR cross-reactivity. The structural alterations in the trimolecular complex are distinct from previously characterized self-reactive TCRs, indicating that there are multiple unusual ways for self-reactive TCRs to bind their pMHC ligand.

CORRESPONDENCE
Kai W. Wucherpfennig:
kai_wucherpfennig@dfci.harvard.edu

Abbreviations used: CDR, complementarity-determining region; EAE, experimental encephalomyelitis; HA, hemagglutinin; MBP, myelin basic protein; MS, multiple sclerosis; pMHC, peptide–MHC.

Self-reactive lymphocytes that escape elimination during development can cause autoimmune diseases later in life. Structural characterization of a substantial number of self-reactive TCRs is necessary to define at a repertoire level how such TCRs can productively engage self-antigen despite the need to escape deletion. Five structures have thus far been determined, involving two human TCRs from multiple sclerosis (MS) patients (Hahn et al., 2005; Li et al., 2005) and three murine TCRs from the experimental encephalomyelitis (EAE) model of MS (Maynard et al., 2005; Feng et al., 2007). The two human TCRs (Ob.1A12 and 3A6) showed a shift toward the peptide N terminus that reduced TCR interaction with HLA-DR (abbreviated as DR)–bound peptides from myelin basic protein (MBP; Hahn et al., 2005; Li et al., 2005; Wucherpfennig et al., 2009). Although three murine TCRs bound with normal topology, they also showed a suboptimal interaction with the self-peptide because only part of the groove was filled by the N-terminal MBP Ac1-11 epitope (He et al., 2002). The MBP Ac1-11 peptide bound with very low affinity to the relevant MHC molecule (I-A^u; Fairchild et al., 1993; Harrington et al., 1998), and in MBP-deficient mice the T cell response to MBP was focused on C-terminal peptides that bound with substantially higher affinity to I-A^u (Harrington et al., 1998). Negative selection of these T cells in wild-type mice thus permitted the Ac1-11 peptide to become immunodominant even though

The Rockefeller University Press $30.00
J. Exp. Med. Vol. 208 No. 1 91-102
www.jem.org/cgi/doi/10.1084/jem.20100725

it only partially occupied the binding groove. These results suggest that the observed structural defects in these trimolecular recognition units are caused by selection events that eliminated self-reactive T cells with optimal TCR binding properties. T cells that expressed the three EAE TCRs were pathogenic (Goverman et al., 1993; Lafaille et al., 1994; Pearson et al., 1997), and transgenic mice that expressed the human Ob.1A12 TCR and the relevant human MHC molecule developed spontaneous CNS inflammation and demyelination (Madsen et al., 1999; Ellmerich et al., 2005). These TCRs thus have altered binding properties that apparently enabled escape from negative selection but still allowed them to bind to their target peptide–MHC (pMHC) complex with sufficient strength to cause disease. The vast majority of antimicrobial TCRs are positioned over the center of the pMHC surface. An N-terminal shift has so far been observed in one case, apparently also as a result of self-tolerance mechanisms (Gras et al., 2009). This TCR (CF34) was specific for an HLA-B8–bound EBV peptide and originated from a person who was HLA-B8 and HLA-B44 heterozygous. The N-terminal shift by this TCR appeared to prevent self-reactivity to HLA-B44. In contrast, the LC13 TCR was alloreactive for HLA-B44 because it was isolated from a person who expressed HLA-B8 but not HLA-B44. This TCR bound over the C-terminal part of the HLA-B8–bound EBV peptide (Gras et al., 2009).

However, the structural database is still too small to adequately describe the recognition properties of self-reactive T cells at a repertoire level, and a substantially larger number of complexes needs to be crystallized to determine to what extent self-reactive TCRs deviate from the rules followed by most antimicrobial TCRs. In particular, the range of possible binding solutions by human autoimmune T cells remains largely unexplored. A large number of crystal structures, as well as functional studies, have shown that antimicrobial TCRs use a diagonal binding mode that positions the four germline-encoded TCR loops (complementarity-determining region [CDR] 1 and CDR2 of TCR-α and -β) over the MHC helices (Sun et al., 1995; Garboczi et al., 1996; Garcia et al., 1996; Garcia and Adams, 2005; Rudolph et al., 2006; Marrack et al., 2008). In most structures, the CDR3 loops also contribute to MHC binding. This binding mode allows the two hypervariable CDR3 loops to make extensive contacts with the bound peptide. In addition, peptide contacts are frequently made by the CDR1α and β loops to N-terminal and C-terminal peptide residues, respectively. A substantial body of recent work has suggested that the observed placement of the germline-encoded CDR1 and CDR2 loops on the MHC helices is the product of coevolution of MHC and TCR genes (Turner et al., 2006; Feng et al., 2007; Dai et al., 2008; Garcia et al., 2009).

Previous studies on human autoimmune TCRs focused on two DR-restricted T cell clones specific for MBP from MS patients. We now report the crystal structure of a human TCR (Hy.1B11) from a relapsing-remitting MS patient that recognizes the same MBP peptide (residues 85–99) as Ob.1A12 TCR but presented by a different MHC molecule, HLA-DQ1 (abbreviated as DQ1). The T cell response to MBP in this patient was dominated by three in vivo expanded T cell clones specific for the MBP_{85-99} peptide that persisted over time. Two of these clones were DR restricted (DRA, DRB1*1602) and one was DQ1 restricted (DQAI*0102, DQBI*0502; Wucherpfennig et al., 1994a,b). A total of three clones with the Hy.1B11 TCR sequence (TRAV13-1*02, TRAJ48*01, and TRBV7-3*01, TRBD2*01, TRBJ2-3*01) were isolated from independent cultures, two from the initial time point and a third 13 mo later (Wucherpfennig et al., 1994b). Furthermore, this T cell clone was activated by four microbial peptides (from herpes simplex virus, adenovirus, human papillomavirus, and pseudomonas) that had limited sequence similarity to the MBP_{85-99} peptide (Wucherpfennig and Strominger, 1995). The structure showed that only one of the two CDR3 loops contacted the bound peptide, explaining why specificity was limited to few peptide residues. This self-reactive TCR thus followed some of the rules established for antimicrobial TCRs (such as binding of the TCR-β chain to the MHC α1 helix) while clearly violating other rules (no MHC helix contacts by TCR-α germline-encoded loops and peptide contacts by only one CDR3 loop). The structure thereby reveals a novel way of self-pMHC recognition by a TCR from a patient with a chronic inflammatory disease.

RESULTS

Unusual features of Hy.1B11 TCR binding to the self-pMHC complex

The complex of Hy.1B11 TCR and DQ1-MBP_{85-99} peptide crystallized in the space group $P2_12_12_1$, and one of the crystals diffracted to a resolution of 2.55 Å. The structure was determined by molecular replacement with one molecule in the asymmetric unit and refined to R_{work}/R_{free} values of 23.2 and 25.8%, respectively. Crystal data and refinement statistics for the structure are shown in Table S1. Excellent electron density was observed at the interface for the CDR loops of the TCR, the peptide, and the DQ1 helices (Fig. S1). The structure showed a strong tilt in TCR binding toward the DQ1 α1 helix, which prevented interaction of the TCR Vα chain with the DQ1 β1 helix (Fig. 1, a, c, and e). The tilt was 14.5° compared with the influenza hemagglutinin ($HA_{306-318}$)-specific HA1.7 TCR (Hennecke et al., 2000; Fig. 1, b, d, and f), measured using a vector through the centers of mass of the Vα and Vβ domains. In addition, a small crossing angle (40°) of the TCR over the pMHC surface was observed which apparently prevented MHC engagement by the CDR1β loop. This crossing angle was smaller than for any other studied MHC class II restricted TCR (Fig. S2), but a similar crossing angle had been observed for the MHC class I restricted 2C TCR (Garcia et al., 1998; Rudolph et al., 2006). As a result of the tilt and the small crossing angle, the center of mass of the Vα domain was shifted toward the peptide by ∼6 Å compared with HA1.7, and the center of mass of the Vβ domain was also shifted by ∼6.5 Å (Fig. S2). The tilted position resulted in limited Hy.1B11 TCR interaction with the DQ1 β1 helix (Table I) and also substantially reduced TCR interactions

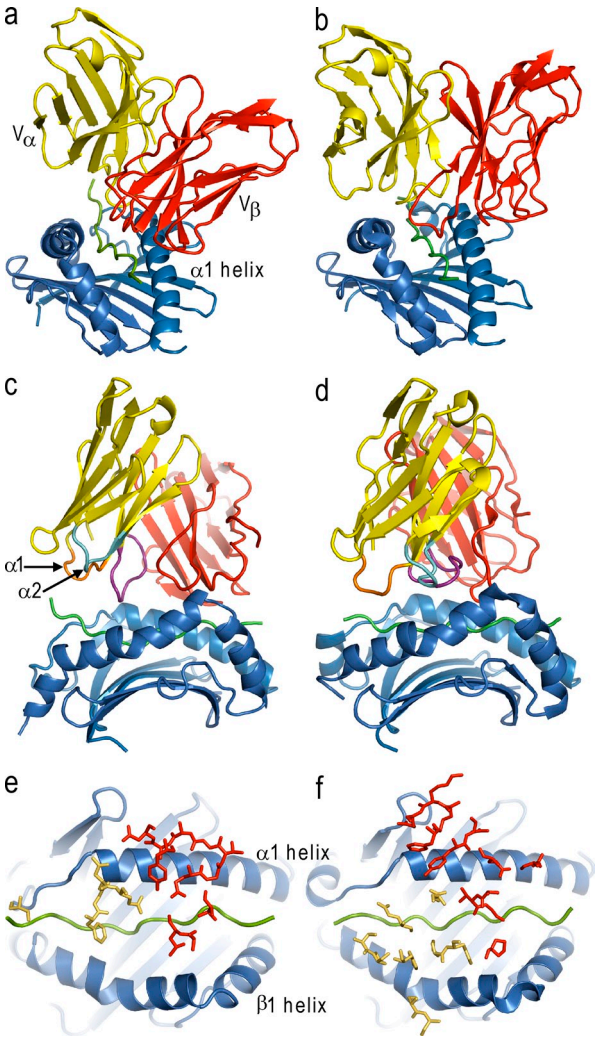

Figure 1. The highly tilted Hy.1B11 TCR binding mode prevents MHC contact by the germline-encoded TCR-α chain loops. The self-reactive Hy.1B11 TCR (a, c, and e) is compared with the influenza HA-specific HA1.7 TCR (b, d, and f). The TCR-α and -β variable domains are colored in yellow and red, respectively, the MHC molecules in blue, and peptides in green. TCR and MHC constant domains have been omitted for clarity. The trimolecular complexes formed by Hy.1B11 and HA1.7 TCRs are viewed from the peptide C terminus (a and b) and rotated by 90° (c and d). The CDR1α and CDR2α loops of Hy.1B11 TCR are labeled (c). CDR1α (α1) is colored orange, CDR2α (α2) cyan, and CDR3α purple. Hy.1B11 (e) and HA1.7 (f) TCR residues that contact the respective pMHC complex are colored yellow for TCR-α and red for TCR-β.

with the peptide (Fig. 1 e), as discussed below in greater detail. In contrast, HA1.7 TCR made a large number of contacts with both MHC helices and the HA peptide (Fig. 1 f). The total buried surface area of the complex was 1645 Å^2, of which approximately half was contributed by TCR and pMHC, respectively. Overall, the peptide contributed 36% of the pMHC buried surface area, with the remainder contributed by the MHC protein. The TCR-α chain contributed almost half (44%) of the total buried surface area, but 85% of the surface area buried by the TCR-α chain was contributed by the CDR3α loop because the CDR1α and CDR2α loops did not bind to DQ1.

Table I. Contacts of Hy.1B11 TCR with HLA-DQ1

CDR	TCR residue	DQ1 residue	Number of contacts
Contacts of TCR with HLA-DQ1α			
CDR3α	G96	Q57	2
CDR3α	G96	G58*	2
CDR3α	N97	D55	2
CDR3α	N97	Q57	3
CDR3α	E98	R61**	11
CDR2β	Y46	R61	1
CDR2β	Q48	R61	1
CDR2β	Q48	A64	1
CDR2β	Q48	V65	4
CDR2β	G49	H68	3
CDR2β	T50	H68*	4
CDR2β	A52	A64	1
CDR2β	A53	A64	3
CDR2β	A53	R61	1
CDR2β	A53	Q57*	2
CDR2β	A53	L60	1
CDR2β	D54	Q57	4
CDR3β	L95	R61	1
Contacts of TCR with HLA-DQ1β			
CDR3β	A94	E66	3
CDR3β	L95	E66	2

*, Putative hydrogen bond; **, two putative hydrogen bonds.

Only a single germline-encoded Hy.1B11 TCR loop binds to HLA-DQ1

Four germline-encoded TCR loops, CDR1 and CDR2 of both TCR chains (Fig. 2 b, yellow), and both CDR3 loops (Fig. 2 b, red) typically contact the MHC helices, as illustrated for the human HA1.7 TCR (Hennecke et al., 2000). In stark contrast, only a single germline-encoded loop of Hy.1B11 TCR (CDR2β) bound to DQ1 (Fig. 2 a). There were no contacts between the TCR Vα domain and the DQ1 β1 helix, and only a single residue on the DQ1 β1 helix (E66) was contacted by Hy.1B11 TCR (through CDR3β; Fig. 2 e and Table I). Hy.1B11 TCR thus formed extensive interactions with the DQ1 α1 helix but only limited contacts with the DQ1 β1 helix (Fig. 2, c and e), whereas HA1.7 TCR had extensive interactions with both MHC helices (Fig. 2, d and f). The absence of MHC binding by three of the germline-encoded TCR loops was partially compensated by both CDR3 loops, in particular CDR3α, which made a substantial number of contacts with the DQ1 α1 helix (Table I; Fig. 2, c and e). Two distinctive features of Hy.1B11 TCR binding were responsible for this highly unusual interaction with the MHC molecule: the tilt that prevented DQ1 binding by the germline-encoded TCR-α loops and a small crossing angle.

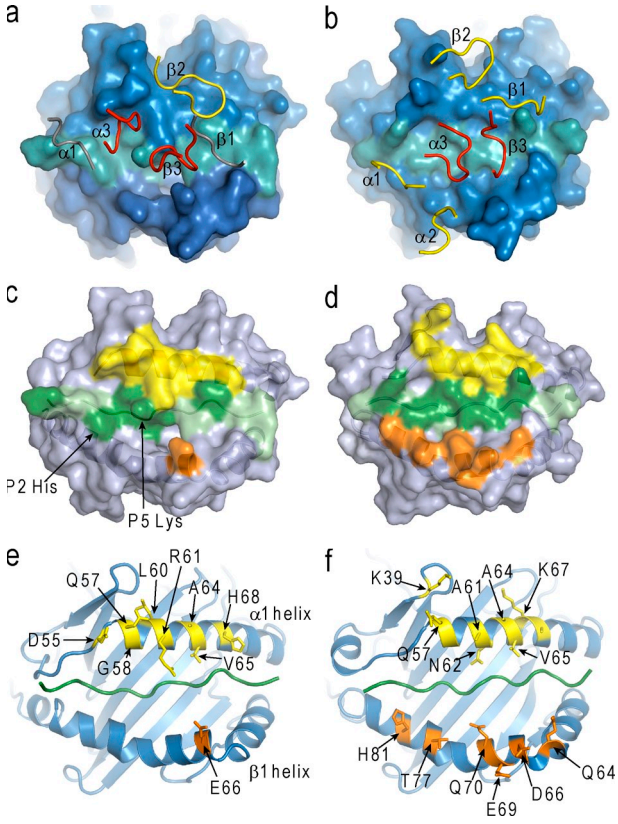

Figure 2. Only a single germline-encoded loop of Hy.1B11 TCR interacts with MHC. The CDR loops that contact the MHC helices are shown for two human MHC class II restricted TCRs (Hy.1B11 and HA1.7; a and b, respectively). The germline-encoded CDR1 and CDR2 loops which contact MHC are colored yellow, hypervariable CDR3 loops red, and CDR1/CDR2 loops contacting only peptide gray. Only loops making contact with MHC or peptide are shown. MHC class II molecules are rendered as a surface colored in blue. Peptides are colored teal. TCR-α CDR loops are labeled as α1, α2, and α3, and TCR-β loops as β1, β2, and β3. Footprint of TCR Hy.1B11 (c) and HA1.7 (d) on their pMHC ligand is shown. MHC is rendered as a surface. TCR contacts with the MHC α1 helix are colored yellow, and MHC β1 helix orange. Peptide surfaces are colored light green. Peptide residues contacted by TCR are colored dark green. Contacts with the MHC helices made by Hy.1B11 (e) and HA1.7 TCR (f) are colored yellow for the MHC class II α1 helix and orange for the MHC class II β1 helix.

The tilt prevented engagement of CDR1α and CDR2α, and the small crossing angle shifted CDR3α toward the DQ1 α1 helix. This TCR thus represents the first example in which the MHC molecule is recognized by only one of the four germline-encoded TCR loops.

Positioning of the Hy.1B11 CDR2β loop on DQ1

Despite these highly unusual features, the Hy.1B11 TCR was positioned diagonally on the pMHC complex similar to other TCRs. The CDR2β loop contributed >70% of the surface area buried by the TCR-β chain, and we therefore examined its interaction with the DQ1 α1 helix in detail. Crystallographic studies of TCRs that used Vβ8.2 identified a common binding mode of the CDR2β loop on the MHC class II α1 chain helix (Fig. 3 d, showing B3K506 TCR as an example; Feng et al., 2007; Dai et al., 2008; Garcia et al., 2009). Furthermore, mutation of this loop in TCR-β single chain transgenic mice interfered with T cell development (Scott-Browne et al., 2009). Comparison of Hy.1B11 TCR, two other human TCRs (HA1.7 and 3A6), and the mouse B3K506 TCR (as well as four other investigated TCRs; not depicted) showed a similar overall positioning of this CDR2β loop on the MHC class II α1 helix (Fig. 3, a–d; Marrack et al., 2008). Among all four TCRs, CDR2β residues 48 and 54 contacted the same positions on the MHC class II α1 helix (positions 61 and 57, respectively; Fig. 3 e), even though many of the interacting MHC and TCR side chains were chemically different. In addition, CDR2β residue 46 of Hy.1B11 and B3K506 TCRs interacted with residue 61 on the MHC α1 helix, whereas CDR2β residue 53 of both Hy.1B11 and 3A6 TCR bound to positions 57 and 61 on the MHC. Although the

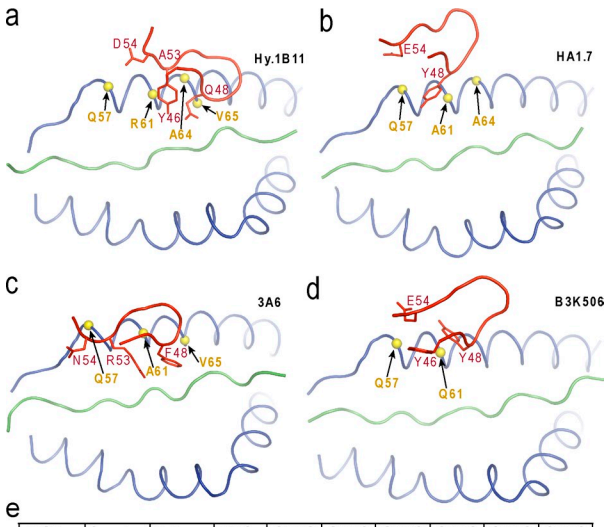

e

TCR	Species	Antigen	MHC	CDR2 β46	CDR2 β48	CDR2 β49	CDR2 β50	CDR2 β53	CDR2 β54
Hy.1B11	Human	MBP	DQ1	Y R61	R61 Q A64 V65	G H68	T H68	Q57 A L60 R61 A64	D Q57
HA1.7	Human	HA	DR1	F Q57	Q57 Y G58 A61 A64	A64 D K67	V	K K39	E K39 Q57
3A6	Human	MBP	DR2a	E	A61 F V65	A61 N V65	E	Q57 R G58 A61	Q57 N E55
B3K506	Mouse	3K	I-A^b	Q57 Y Q61	Q57 Y L60 Q61	V	A	T	E Q57

Figure 3. The overall placement of the Hy.1B11 CDR2β loop on the MHC class II α1 helix is similar to other structures. The placement of the CDR2β loop of Hy.1B11 TCR (a) on the MHC class II α1 helix is compared with two other human TCRs (HA1.7 and 3A6; b and c, respectively) and a murine TCR (B3K506, d). MHC class II residues on the α1 helix contacted by multiple TCRs are highlighted as yellow spheres. The CDR2β loop is colored red and only side chains making contact to the MHC molecule are shown. CDR2β residues, as well as interacting MHC α1 helix residues, are listed (e). Contacts made by multiple TCRs are highlighted in yellow.

overall positioning of the β2 loops on the MHC class II α1 helix was similar, the molecular details of the interactions were distinct as a result of differences in docking angles, MHC polymorphisms, and the actual sequences of the TCR CDR2β loops.

Only one of the CDR3 loops interacts with the MBP peptide

In most previously examined complexes of TCR and pMHC, both CDR3 loops contacted the bound peptide (as exemplified by HA1.7 TCR; Fig. 4 b). CDR3β apparently could not contact the DQ1-bound peptide because of its short length and the unusual tilt of Hy.1B11 TCR. The Hy.1B11 CDRβ3 loop was 10 amino acids in length compared with 9–16 amino acids in other TCR structures (Table S2). The majority of peptide contacts were instead made by the CDR3α loop, in particular F95α (TRAJ48), which was inserted deeply between the P2 His and P3 Phe side chains of the peptide (Fig. 4 a and Table II). Furthermore, the main chain carbonyl of F95α formed a hydrogen bond with P5 Lys of the peptide. Only one other residue of this CDR3 loop, E98α, contributed to peptide recognition through two contacts with P5 Lys. Functional experiments using a set of single amino acid analogue peptides confirmed that peptide specificity of the Hy.1B11 T cell clone was limited to the P2 to P5 peptide segment to which the CDR3α loop bound. All alanine analogues within this segment showed a substantial reduction in T cell proliferation at a low peptide concentration (100 nM; Fig. 5 a). However, only the alanine substitution of P5 Lys resulted in a complete loss of activity at a higher peptide concentration (1 μM; Fig. 5 b), suggesting an energetically important contribution of bonds made to the P5 Lys sidechain. TCR specificity for the four peptide positions in the P2 to P5 segment was further investigated using a panel of single amino acid analogues for each position that represented all naturally occurring amino acids except cysteine (Fig. 5, c–f). Consistent with the structural data, the highest degree of specificity was observed for P3 Phe and P5 Lys, which showed a preference for hydrophobic and basic amino acids, respectively (Fig. 5, d and f). In contrast, more than half of the analogues of P2 His showed stimulatory activity (Fig. 5 c). An analogue with a phenylalanine-to-glycine substitution at P3 was active, possibly as a result of new contacts enabled by the well-established flexibility of CDR3 loops (Fig. 5 d; Garcia et al., 1998). P4 Phe represented an anchor residue for DQ1 binding that was deeply buried in the DQ1 binding groove (Fig. S3). This pocket had a preference for large hydrophobic residues, but smaller hydrophobic residues and histidine were also tolerated (Fig. 5 e). In the structure, a few contacts were also made to peptide positions P-3 Asn (by CDR1α) and P8 Val (by CDR1β and CDR2β). These contacts were mediated through the peptide backbone. Consistent with this fact, substitution of these peptide residues by alanine did not reduce activity. These data thus support the functional relevance of the structural data and demonstrate that the majority of functionally important peptide contacts are made by a single TCR loop, CDR3α.

Table II. Contacts of Hy.1B11 TCR with the MBP_{85-99} peptide

CDR	TCR residue	Residue of peptide	Number of contacts
Contacts to peptide by TCR-α chain			
CDR1α	S28#	P-3 Asn	1
CDR3α	F95	P2 His	15
CDR3α	F95	P3 Phe	7
CDR3α	F95*	P5 Lys	3
CDR3α	E98	P5 Lys	2
Contacts to peptide by TCR-β chain			
CDR1β	Thr28	P8 Val	2
CDR2β	Gln48	P8 Val	2
CDR2β	Gly49	P8 Val	3

Putative hydrogen bond to peptide sidechain (*) or to peptide backbone (#).

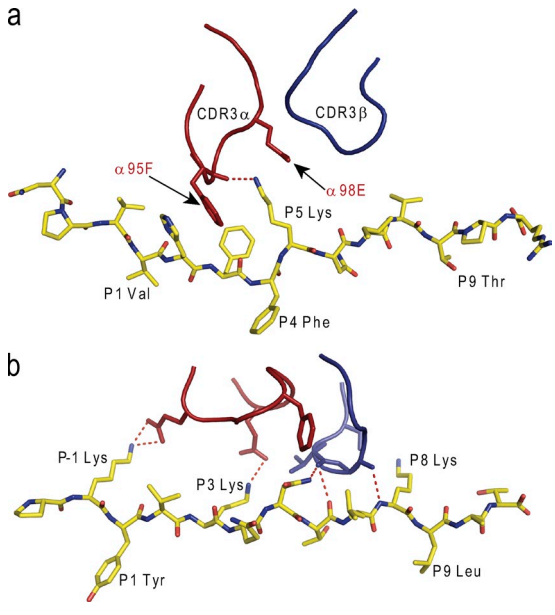

Figure 4. Only one of the Hy.1B11 CDR3 loops interacts with the peptide. The interaction of the CDR3 loops with peptide is compared for TCRs Hy.1B11 (a) and HA1.7 (b). CDR3α (red) and CDR3β (blue) are represented as loops, and side chains interacting with the peptide are shown. Hydrogen bonds are indicated as red dashes.

Intermediate binding affinity of Hy.1B11 TCR

Surface plasmon resonance measurements were performed to compare the binding affinity of the MBP_{85-99}-specific Hy.1B11 and Ob.1A12 TCRs for their ligands (DQ1-MBP_{85-99} and DR2-MBP_{85-99}, respectively). Monobiotinylated pMHC complexes were captured on a streptavidin sensor chip and soluble Hy.1B11 or Ob.1A12 TCR was injected over these surfaces. Hy.1B11 TCR bound to DQ1-MBP_{85-99} with a K_d of 14.3 μM based on equilibrium binding data (Fig. 6 b and Fig. 7 b). In contrast, the affinity of Ob.1A12 TCR for DR2/MBP_{85-99} was lower, at ~100 μM (our measurements; Cole et. al., 2007). Hy.1B11 TCR binding was specific because a control TCR (Ob.1A12) showed no binding to DQ1-MBP_{85-99}

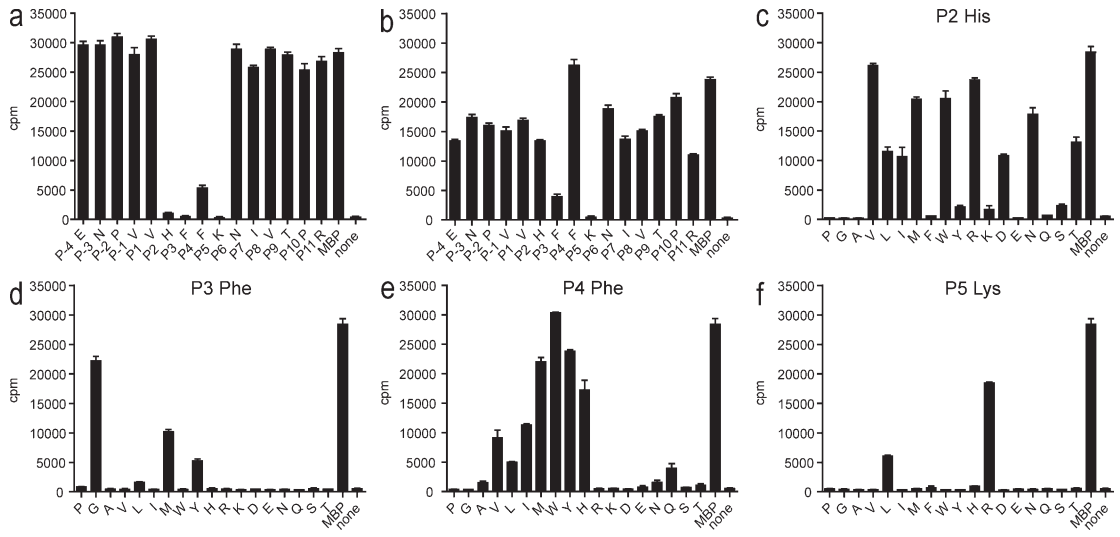

Figure 5. Specificity of TCR recognition is limited to a short segment of the MBP peptide. T cell proliferation induced by a panel of single amino acid alanine analogues of the MBP_{85-101} peptide (indicated as P-4 to P11 for each position in the MBP_{85-99} region) as well as the native MBP_{85-101} peptide at concentrations of 100 nM (a) or 1 µM (b). Four peptide positions with reduced responses to the alanine analogues (P2 His, P3 Phe, P4 Phe, and P5 Lys) were further examined with a set of 18 single amino acid analogue peptides representing all naturally occurring amino acids (except cysteine) in a T cell proliferation assay at a concentration of 100 nM (c–f). T cell proliferation was measured by [^{3}H]-thymidine incorporation using EBV-transformed B cells expressing DQ1 as antigen-presenting cells. Experiments were independently performed twice with similar results. Additional experiments performed with smaller sets of peptides also confirmed the conclusions. The data represent the mean and standard deviation of triplicate measurements.

(Fig. S4) and Hy.1B11 TCR did not bind to either DQ1-CLIP or DR2/MBP_{85-99} control complexes (not depicted). Consistent with these affinity measurements, Hy.1B11 TCR had a higher shape complementarity (0.63) than Ob.1A12 TCR (0.51) for its pMHC ligand, whereas the solvent inaccessible area was in a similar range for both TCRs (1,645 and 1,688 Å^2 for the complexes formed by Hy.1B11 and Ob.1A12 TCRs, respectively). Greater shape complementarity can result in higher affinity (Garcia et al., 1998; Reinherz et al., 1999), but it remains unknown whether this aspect explains the moderately higher affinity of Hy.1B11 compared with Ob.1A12 TCR.

The differences in binding affinities between Hy.1B11 and Ob.1A12 may be related to differences in HLA-DQ and HLA-DR expression levels and patterns. Histological studies showed very low expression of HLA-DQ in the thymic medulla, the site of negative selection, whereas HLA-DR protein could be readily detected (Ishikura et al., 1987). It is also well known that HLA-DQ molecules are expressed at substantially lower levels (~10-fold) than HLA-DR molecules on peripheral antigen-presenting cells (Roucard et al., 1996). Direct comparison of Hy.1B11 and Ob.1A12 T cell clones showed that Hy.1B11 T cells required higher concentrations of MBP_{85-99} peptide for stimulation, despite the higher affinity of Hy.1B11 TCR for its pMHC ligand (Wucherpfennig et al., 1994a). The higher affinity of Hy.1B11 compared with Ob.1A12 TCR may therefore compensate for the substantially lower level of HLA-DQ than HLA-DR expression.

Mutagenesis of MHC and peptide contacts

Given this unusual binding topology, alanine scanning mutagenesis was performed to validate the structure and to define

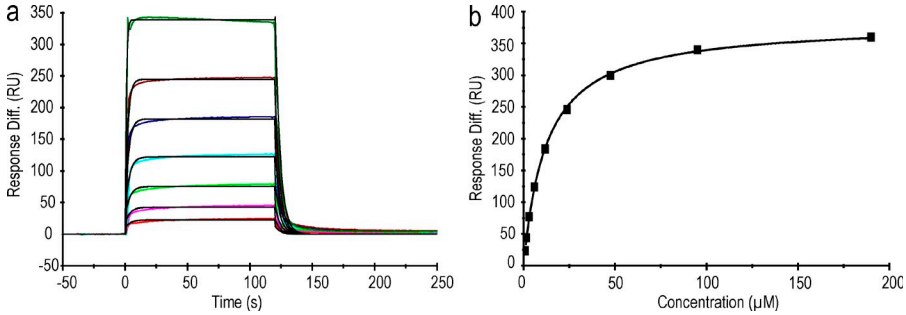

Figure 6. Hy.1B11 TCR binds with an intermediate affinity to the DQ1–MBP peptide complex. (a) Different concentrations of monomeric Hy.1B11 TCRs (0.75, 1.5, 3, 6, 12, 24, and 96 µM) were injected over a flow cell with immobilized DQ1-CLIP (700 RU), followed by a flow cell with immobilized DQ1-MBP_{85-99} (700 RU) at a flow rate of 15 µl/min. TCR was injected for 2 min at 25°C. The signal from the DQ1-CLIP reference flow cell was subtracted from the DQ1-MBP_{85-99} flow cell and data were fitted to a 1:1 (Langmuir) binding model using BIAevaluation software. (b) For equilibrium binding analysis nine serial dilutions were injected using the same setup as in (a), and the equilibrium-binding constant K_d was calculated using a nonlinear curve fit. The experiment was independently performed at least twice with similar results.

key TCR contact residues for DQ1 and the MBP_{85-99} peptide. All TCR residues that contacted DQ1 were mutated to alanine, except native alanine or glycine residues. In addition, CDR3α F95 was mutated to alanine, given its central role in peptide recognition (Fig. 7, a and b). For each mutant, nine concentrations were tested under equilibrium binding conditions to obtain reliable affinity measurements (Fig. S5). As a control, a double mutant of two noncontacting residues in CDR1α and CDR2α (N31A and S52A) was generated. This double mutant showed an affinity to DQ1-MBP_{85-99} close to wild-type Hy.1B11 TCR (13.8 and 14.3 μM, respectively). Four of the nine mutants had greatly reduced affinities for DQ1-MBP_{85-99}, and these targeted TCR residues made contacts solely to DQ1 (CDR3β L95A, 110 μM), to both DQ1 and MBP_{85-99} peptide (CDR2β Q48A, 108 μM; and CDR3α E98A, >250 μM), or only the peptide (CDR3α F95A, >250 μM). These mutagenesis data also showed that the unusual TCR binding mode was not a crystallization artifact.

a

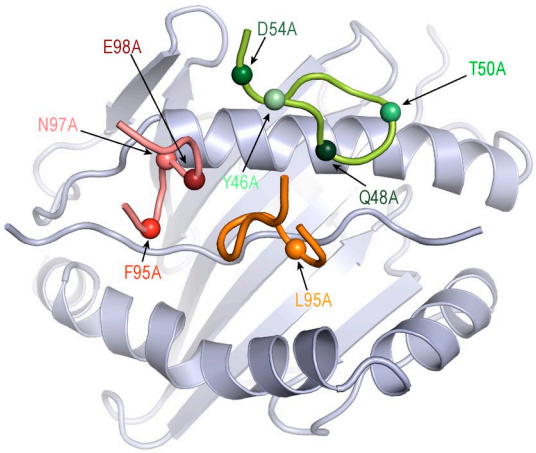

b

	TCR mutant	K_d (μM) (Equilibrium)	Contacts		No. of contacts disrupted
			HLA-DQ1	Peptide	
	Wild type	14.3 ± 1.5			
CDR2β	Y46A	15.8 ± 0.9	1	0	1
	Q48A	108.0 ± 4.0	6	2	5
	T50A	20.0 ± 1.2	4 (1)	0	2
	D54A	30.8 ± 2.6	4	0	3
CDR3β	L95A	110 ± 6.0	3	0	2
CDR3α	F95A	>250	0	25 (1)	23
	N97A	38.0 ± 6.0	5	0	4
	E98A	>250	11 (2)	2	13 (2)
CDR1α & CDR2α	N31A & S52A	13.8 ± 0.7	0	0	0

Figure 7. TCR mutagenesis identifies key contact residues in the CDR2β and CDR3 loops. (a) TCR point mutants are shown as colored balls: mutations in CDR2β in shades of green, CDR3α mutants in shades of red, and the CDR3β mutant in orange. Darker colors indicate stronger effects of mutations. pMHC is shown as a cartoon in silver. (b) Table showing the equilibrium binding affinity constants of TCR mutants. The number of contacts made to peptide or MHC by each residue are enumerated, along with the number of contacts disrupted by substitutions with alanine. Hydrogen bonds are indicated in parentheses. The equilibrium binding experiments were performed at least twice.

Binding by the CDR2β loop involved a combination of side chain and main chain contacts (Table I). The Q48A mutant showed substantially reduced DQ1-MBP_{85-99} binding (108 μM; Fig. 7 b). However, the binding contribution from two main chain hydrogen bonds (CDR2β Thr 50–DQ1α His 68 and CDR2β Ala 53–DQ1α Gln 57) could not be assessed with these mutants (Table I), which made it difficult to determine the total contribution of this TCR loop to DQ1 binding.

In contrast, CDR3α contacts were predominantly made by side chains. CDR3α E98A and F95A mutations resulted in a severe reduction in binding (>250 μM for both mutants). CDR3α F95 formed the majority of peptide contacts, and mutation to alanine greatly reduced TCR binding affinity for DQ1-MBP_{85-99}. Nevertheless, this mutation did not assess the entire contribution by F95 because it did not eliminate the hydrogen bond between the main chain of F95 and the peptide side chain P5 Lys. The CDR3α E98A mutation resulted in the most substantial reduction in DQ1-MBP_{85-99} binding because of loss of two hydrogen bonds to DQ1α R61 and 11 other contacts, including two contacts to P5 Lys of the peptide.

CDR3β made no contacts to the peptide and only limited contact to the DQ1β helix. CDR3β L95 contacted DQ1β E66, and the L95A mutant showed a substantial reduction in affinity (110 μM). The interaction of CDR3β with the DQ1β helix also involved water-mediated hydrogen bonds. DQ1β E66 hydrogen bonded with a water molecule, which, in turn, hydrogen bonded with CDR3β main chain (S93, A94, L95, and E96) and side chain (D97) residues. It is possible that this hydrogen bonding network was destabilized by the CDR3β L95A mutation.

The mutagenesis data showed that all three TCR loops that contacted the DQ1 helices in the crystal structure contributed to DQ1 binding in this functional assay. The data also highlighted the critical energetic role of the CDR3α loop in binding to the DQ1-MBP_{85-99} complex, in particular the important contributions by CDR3α F95 and E98, which made many contacts to the peptide (CDR3α F95) and DQ1 (CDR3α E98) in the structure.

DISCUSSION

Autoaggressive T cells have to meet two competing requirements: they have to escape negative selection in the thymus, yet they need to be capable of initiating TCR signals of sufficient strength upon recognition of the self-antigen in the target organ of the disease. The prior structural characterization of two human TCRs from MS patients (Hahn et al., 2005; Li et al., 2005) and of three mouse TCRs from the EAE model (Maynard et al., 2005; Feng et al., 2007) showed in each case significant structural alterations that impaired TCR binding to the MHC-bound self-peptide (Wucherpfennig et al., 2009). The human TCRs bound with an altered topology, whereas the mouse TCRs bound with a normal topology. However, in all cases the interaction with the peptide was compromised either because of a shift in TCR binding (human TCRs) or partial occupancy of the peptide binding groove (murine TCRs). The structure of the self-reactive Hy.1B11 TCR

represents the first case in which only one of the four germline-encoded TCR loops interacts with the MHC helices. Furthermore, only one of the CDR3 loops interacts with the peptide, limiting TCR specificity to a short peptide segment (P2 His, P3 Phe, and P5 Lys). The structure thus explains how Hy.1B11 TCR responds to multiple microbial peptides that share limited sequence similarity with MBP_{85-99}, in particular P3 Phe, a basic residue at P5, and hydrophobic anchors at P1 and P4 (Fig. S6; Wucherpfennig and Strominger, 1995).

The Hy.1B11 and Ob.1A12 TCRs recognize the MBP_{85-99} peptide bound in the same register to DQ1 and DR2, respectively (Fig. S3). The structures of the bound peptides are thus quite similar, except that the P4 Phe side chain is positioned deeper in the hydrophobic P4 pocket of DQ1 (Fig. S3 c). Interestingly, specificity of both TCRs is focused on the P2, P3, and P5 peptide sidechains, but through different structural mechanisms; Ob.1A12 TCR is shifted toward the peptide N terminus, which centers the CDR3 loops over P2 His, whereas Hy.1B11 is positioned over the center of the peptide binding groove but recognizes peptide side chains only through CDR3α and not CDR3β. It is possible that both TCRs bind to this peptide segment because it is more firmly anchored in the peptide binding groove, whereas the C-terminal part of the MBP_{85-99} peptide is raised in both structures (Fig. S3 c; Smith et al., 1998). In both cases, the TCR contacts one of the MHC helices in the typical location, either the MHC class II α1 chain helix (Hy.1B11 TCR-β chain with CDR2β loop) or the MHC class II β1 helix (Ob.1A12 TCR-α chain with CDR1α and CDR2α loops; Fig. S7). However, the germline-encoded loops of the other TCR chain either do not engage the MHC molecule (Hy.1B11) or bind in a highly unusual location (Ob.1A12).

In the majority of previously determined structures, all four germline-encoded loops contact the MHC helices (21 of 29 structures, with each TCR counted only once using the structure with the principal pMHC ligand; Rudolph et al., 2006; Marrack et al., 2008; Garcia et al., 2009). These include 12 of 17 structures involving MHC class I and 9 of 12 structures involving MHC class II molecules. In seven structures, three germline-encoded TCR loops interact with the MHC helices (four MHC class I and three MHC class II restricted TCRs). These seven include two human self-reactive TCRs (Ob.1A12, 3A6) with a shifted binding topology toward to the peptide N terminus (Hahn et al., 2005; Li et al., 2005). In each of these seven cases, one of the CDR3 loops contacts both MHC helices. The A6 TCR that recognizes a HLA-A2–bound HTLV-1 Tax peptide uses the CDR1α and CDR2α loops to bind to the HLA-A2 α2 helix, but the CDR1β and CDR2β loops do not contact the HLA-A2 α1 helix (Garboczi et al., 1996). However, the CDR3β loop has a large footprint and interacts with both MHC α1 and α2 helices. In addition, both MHC helices are contacted by the CDR1α loop. This large structural database permits the conclusion that the interaction of Hy.1B11 TCR with its MHC molecule is unusual.

There are now several examples in which there are unusual features of peptide recognition, such as TCR binding to peptides bulging out of the MHC class I binding groove. A super-bulged 13-amino peptide bound to HLA-B*3508 is recognized by SB27 TCR and the interface is dominated by TCR–peptide interactions. Nevertheless, each of the four germline-encoded TCR loops contacts the MHC protein, even though these interactions are limited (Tynan et al., 2005). In another example, the ELS4 TCR flattens a peptide bulging out of the groove of HLA-B*3501, which enables more extensive MHC contacts. Again, all four germline-encoded loops are involved in MHC binding (Tynan et al., 2007). The BM3.3 TCR shows cross-reactivity between VSV8 and pBMI peptides bound to H-$2K^b$, and there are large differences in the contribution of the Vα and Vβ chains to the interface between the two structures (Reiser et al., 2000). Nevertheless, all four germline-encoded TCR loops contribute to MHC recognition in both complexes.

The YAe62 TCR was isolated from mice in which negative selection was severely limited by expression of a single MHC class II–peptide complex in the thymus (Huseby et al., 2005). Even though YAe62 TCR contacts both MHC helices, it has a substantially larger interaction surface with the α1 than the β1 helix of the MHC molecule because of a tilt in TCR binding (Dai et al., 2008). Unbalanced TCR interactions with the two MHC helices can thus occur in T cells that were either not subjected to negative selection (YAe62 TCR) or escaped elimination in the thymus (Hy.1B11 TCR). Furthermore, there are now three TCRs that recognize the bound peptide using only one CDR3 loop: YAe62 and BM3.3 TCRs with their CDR3β loops and Hy.1B11 with its CDR3α loop (Reiser et al., 2000; Dai et al., 2008). The YAe62 TCR is extremely cross-reactive to both peptide and MHC variants, and the BM3.3 TCR was shown to cross react with a viral octapeptide presented by H-$2K^b$. Peptide recognition by a single CDR3 loop is therefore also unusual within the large structural database that is now available.

The importance of the germline loops of both TCR chains in MHC restriction has been repeatedly demonstrated using mutagenesis approaches and analysis of natural MHC micropolymorphisms (Sim et al., 1996; Manning et al., 1998; Wu et al., 2002; Huseby et al., 2006). Recent structural and functional studies strongly support the hypothesis that the conventional diagonal TCR binding mode is the result of coevolution between MHC and TCR genes (Turner et al., 2006; Feng et al., 2007; Dai et al., 2008; Marrack et al., 2008; Garcia et al., 2009). The diagonal binding orientation on the pMHC surface is similar among most crystallized αβ TCRs, but because of variation in the binding angle it has not been possible to identify conserved MHC residues contacted by all TCRs (Baker and Wiley, 2001; Rudolph et al., 2006). However, seven crystal structures involving six different Vβ8.2 TCRs and one Vβ8.1 TCR that bound mouse I-A molecules showed a close convergence of CDR1β and CDR2β contacts with the I-A α1 helix (Garcia et al., 2009). These results suggest that particular V domains have preferred binding sites on the MHC helices. In mice with a single rearranged TCR-β chain, mutation of the CDR2β residues Tyr46 or Tyr48 to

alanine caused a substantial reduction in the number of thymocytes. Furthermore, these mutations changed Vα usage, which is apparently a compensatory mechanism to enable positive selection of some T cells despite reduced MHC binding by the Vβ chain (Scott-Browne et al., 2009). Studies on MHC class I restricted TCRs have also identified MHC residues that are frequently recognized by TCRs, but the contribution of these MHC residues to binding differs among individual TCRs (Burrows et al., 2010).

CDR2β residues of Hy.1B11 were found to interact with a similar set of MHC positions as other MHC class II restricted TCRs. Given that CDR2β is the only germline-encoded TCR loop that contacts DQ1, it is possible that the placement of this loop on the DQ1 α1 helix contributed to the diagonal position of this TCR over the center of the DQ1-MBP_{85-99} surface. Alanine scanning mutagenesis showed that the two CDR3 loops contributed significantly to DQ1 binding. CDR3 loops have been shown to be flexible (Garcia et al., 1998; Hare et al., 1999; Armstrong et al., 2008) and, in addition to contacting the peptide, they can make important contributions to MHC binding (Garboczi et al., 1996; Borg et al., 2005). The orientation of Hy.1B11 TCR on the DQ1-MBP_{85-99} surface therefore appears to result from the combined binding contributions of the CDR2β and both CDR3 loops.

The unusual structure of the Hy.1B11 TCR–DQ1-MBP_{85-99} complex also raises the important question of how the corresponding human T cell escaped from negative selection in the thymus, but caution has to be used to extrapolate from structural data to complex in vivo events. This TCR has a higher affinity for its pMHC target than the previously crystallized self-reactive TCRs Ob.1A12 and 3A6 (Hahn et al., 2005; Li et al., 2005). However, the Hy.1B11 TCR is HLA-DQ restricted, whereas the other two TCRs are HLA-DR restricted. HLA-DQ molecules are expressed at ∼10-fold lower levels than HLA-DR molecules (Roucard et al., 1996), and the higher affinity of Hy.1B11 TCR may therefore be required for this TCR to adequately respond to the self-peptide on peripheral antigen-presenting cells. HLA-DQ molecules are expressed at very low levels in the medulla of the thymus (Ishikura et al., 1987), which may have facilitated escape of negative selection by the Hy.1B11 T cell. It is also possible that the tilted binding mode of Hy.1B11 TCR binding affects formation of higher order structures among TCRs and/or other proteins involved in T cell activation at the immunological synapse.

In summary, this self-reactive TCR interacts in an unusual manner with both the self-peptide and the MHC molecule. The binding mode differs substantially from the other two autoimmune TCRs that have been crystallized, demonstrating that there are multiple unusual ways for self-reactive TCRs to bind their pMHC ligand. Particularly intriguing is the limited interaction surface with the self-peptide and the functional relevance of this finding for the activation of this self-reactive T cell clone by microbial peptides.

MATERIALS AND METHODS

Protein expression and complex formation. Hy.1B11 TCR used the gene segments TRAV13-1*02, TRAJ48*01 (non-nucleotide–encoded sequence, *g*; CDRα3 protein sequence, AASSFGNEKLT) and TRBV7-3*01, TRBD2*01, TRBJ2-3*01 (non-nucleotide–encoded sequence, cctcggccct; CDβ3 protein sequence, ATSALGDTQY). In the expression construct, the MBP_{85-99} peptide was attached to the N terminus of the TCR-β chain through a flexible octapeptide linker (GGSGGGGG), as reported by Hennecke et al. (2000). The interchain disulfide bond located at the C terminus of the Cα and Cβ Ig domains was moved to the N-terminal part of these domains (replacement of Cα Thr48 and Cβ Ser57 with cysteines) to enhance refolding of TCR heterodimer (Boulter et al., 2003). The chains were separately cloned into pET-22b vector (Novagen), and inclusion bodies produced in BL21(DE3) *E. coli* cells (Novagen) were dissolved in 6 M guanidine hydrochloride, 10 mM dithiothreitol, and 10 mM EDTA. To initiate refolding, TCR-α and -β chains were diluted at a 1:1 molar ratio to a concentration of 25 μg/ml of each chain in a refolding buffer containing 4.5 M urea, 0.55 M L-arginine–HCl, 100 mM Tris-HCl, pH 8.2, 1 mM of reduced glutathione (GSH), and 0.1 mM of oxidized glutathione (GSSH). After 40 h at 4°C, the refolding mixture was dialyzed twice against deionized water and twice against 10 mM Tris-HCl, pH 8.0. Refolded TCR was purified by anion exchange chromatography using Poros PI (Applied Biosystems) and MonoQ (GE Healthcare) columns. TCR mutants were generated by overlapping PCR and cloned into the pET-22b vector (Novagen). These mutant proteins were refolded and purified using the same procedure as wild-type TCR Hy.1B11.

DQ1 was produced in glycosylation-deficient Lec3.2.8.1 cells (Stanley, 1989). The CLIP peptide was attached to the N terminus of the DQ1β chain using a linker with a thrombin cleavage site, and the two chains were cloned into a vector that drives expression of glutamine synthetase to enable selection of transfected clones in glutamine-deficient media (Day et al., 2003). Stable clones were produced under methionine sulphoximine selection and tested for DQ1 secretion by Western blotting. The clone with the highest DQ1 production level was expanded in a hollow fiber bioreactor (AccuSyst miniMax; Biovest International) and secreted DQ1 was affinity-purified using mAb 9.3.F10 (American Type Culture Collection). Fos and Jun leucine zipper dimerization domains at the C termini used to facilitate DQ1 heterodimer formation were removed by V8 protease cleavage.

After cleavage of the CLIP peptide linker, complexes were formed by permitting binding of the TCR-β chain–linked MBP_{85-99} peptide to the DQ1 binding site. TCR, DQ1, and HLA-DM were incubated at a molar ratio of 6:4:1 for 18 h at 25°C at a pH of 5.4, and the complex was separated from components by gel filtration (Superdex S-200 column; GE Healthcare) and anion-exchange chromatography (MonoQ; GE Healthcare).

Crystallization and data collection. The complex was determined to be pure by SDS-PAGE and isoelectric focusing PAGE. The complex was concentrated to 7.5 mg/ml in 10 mM Hepes, pH 7.2. A crystallization matrix based on conditions in which other TCR–MHC complex crystals were obtained was used as a starting point for screening. Crystals were obtained in multiple conditions. The final crystals for data collection were grown by the hanging-drop vapor-diffusion method against a reservoir of 0.1 M ammonium sulfate, 8–10% PEG 8000, and 50 mM sodium citrate, pH 6.1, at 24°C. Crystals were cryoprotected by the addition of ethylene glycol to 25%. Data were collected at 100 K at the National Synchrotron Light Source at Brookhaven National Laboratories (Upton, New York) using beamline X29 at a wavelength of 1.0 Å by participating in the mail-in program. The data were processed with the HKL2000 program (Otwinowski and Minor, 1997).

Structure determination and refinement. The structure of the complex was determined by molecular replacement using PHASER software (McCoy et al., 2007). A BLAST (Altschul et al., 1990) search of the sequences of TCR Hy.1B11 and DQ1 against the PDB database was used to find the best model for molecular replacement. Separate BLAST searches for TCR-α and -β chains were performed and the TCR with the highest consensus score (PDB accession code 3HG1) was used for molecular replacement. DQ6 (PDB

accession code 1UVQ) was used as the model for DQ1 (Siebold et al., 2004). PHASER gave a clear and unambiguous solution which could be reproduced using the MOLREP program (Vagin and Teplyakov, 1997). Refinement and rebuilding were performed using crystallography and nuclear magnetic resonance system (CNS) and COOT (Emsley and Cowtan, 2004; Brunger, 2007). The overall density was good with the exception of density for residues DQ1α 46–51, which usually form a short ascending loop in most HLA molecules that has been reported to be important for DM engagement. Stereochemical parameters of the structure were evaluated with the PROCHECK program (Laskowski et al., 1993) and found to be within reasonable limits with 91% of the residues in the most favored region and none in the disallowed regions. Buried surface area calculations were done using AREAIMOL (Lee and Richards, 1971) using a probe radius of 1.4 Å. CALCOM (Costantini et al., 2008) was used for all center of mass calculations and all figures were made with PYMOL. Atomic contacts were determined using CONTACT as implemented in CCP4i (CCP4 suite; Collaborative Computational Project, Number 4, 1994); atoms within a 4 Å distance of each other were considered to be in contact. The TCR crossing angle was calculated by drawing a vector between the center of mass of the V_α and V_β domains and measuring the angle as it intersects a line drawn between the P1 and P9 peptide anchor residues. Relative tilt was calculated as in Teng et al. (1998).

Affinity measurements. The interaction of Hy.1B11 TCR with the DQ1–MBP_{85-99} complex was assessed by surface plasmon resonance using a Biacore 3000 instrument (GE Healthcare). DQ1 with a biotinylated C-terminal BirA tag was captured on a Biacore streptavidin chip. After immobilization of ~700, 1,000, or 3,000 resonance units for analysis of TCR binding, solutions containing different concentrations of soluble monomeric wild-type or mutant TCR Hy.1B11 in 10 mM Hepes, 150 mM NaCl, and 0.005% Tween 20 were injected at 15 µl/min at 25°C. Flow cells with DQ1-CLIP or DR2/MBP_{85-99} complexes were used as specificity controls. BIAevaluation version 4.1 was used for all data analysis. Equilibrium K_d values were obtained by nonlinear curve fitting of subtracted curves using the steady-state affinity fitting mode in BIAevaluation version 4.1. K_d values are reported as mean and standard deviation.

Analysis of peptide analogues. Proliferation assays with the Hy.1B11 T cell clone were performed using EBV transformed B cell line 9009 (DQAI*0102, DQBI*0502) as antigen-presenting cells. B cells were irradiated (5,000 rads) and treated with 50 µg/ml mitomycin C (EMD) for 30 min at 37°C. Assays were set up in 96-well U bottom plates with 5×10^4 T cells and 10^4 B cells in 0.2 ml of serum-free AIM-V media supplemented with 2 mM GlutaMAX. Peptides were tested in triplicates at concentrations of 0.1 and 1 µM. After 72 h of co-culture, T cell proliferation was determined by [^{3}H]-thymidine incorporation.

PDB accession no. The coordinates of the Hy.1B11-DQ1–MBP_{85-99} complex have been deposited under PDB accession no. 3PL6.

Online supplemental material. Fig. S1 shows electron density for critical parts of the crystal structure. Fig. S2 shows the center of mass of Vα and Vβ domains of TCR Hy.1B11. Fig. S3 shows that the MBP_{85-99} peptide binds in the same register to DQ1 and DR2. Fig. S4 shows a specificity control for surface plasmon resonance experiments, and Fig. S5 shows equilibrium binding data for the TCR mutants. Fig. S6 shows alignment of microbial peptides that stimulate the Hy.1B11 T cell clone. Fig. S7 shows comparison of the placement of TCR-α germline-encoded loops by the human autoimmune Ob.1A12 TCR and other MHC class II restricted TCRs. Table S1 shows data collection and refinement parameters. Table S2 shows the sequence of CDR3β. Online supplemental material is available at http://www.jem.org/cgi/content/full/jem.20100725/DC1.

This work was supported by grants from the National Institutes of Health (PO1 AI045757 and RO1 AI064177 to K.W. Wucherpfennig) and postdoctoral fellowships from the National Multiple Sclerosis Society (to D.K. Sethi) and the Cancer Research Institute (to D.A. Schubert). Data were collected at beamline X29 of the National Synchrotron Light Source. Financial support for the National Synchrotron Light Source comes principally from the Offices of Biological and Environmental Research and of Basic Energy Sciences of the US Department of Energy, and from the National Center for Research Resources of the National Institutes of Health.

The authors declare no competing financial interests.

Submitted: 14 April 2010
Accepted: 19 November 2010

REFERENCES

Altschul, S.F., W. Gish, W. Miller, E.W. Myers, and D.J. Lipman. 1990. Basic local alignment search tool. *J. Mol. Biol.* 215:403–410.

Armstrong, K.M., K.H. Piepenbrink, and B.M. Baker. 2008. Conformational changes and flexibility in T-cell receptor recognition of peptide-MHC complexes. *Biochem. J.* 415:183–196. doi:10.1042/BJ20080850

Baker, B.M., and D.C. Wiley. 2001. alpha beta T cell receptor ligand-specific oligomerization revisited. *Immunity.* 14:681–692. doi:10.1016/S1074-7613(01)00160-1

Borg, N.A., L.K. Ely, T. Beddoe, W.A. Macdonald, H.H. Reid, C.S. Clements, A.W. Purcell, L. Kjer-Nielsen, J.J. Miles, S.R. Burrows, et al. 2005. The CDR3 regions of an immunodominant T cell receptor dictate the 'energetic landscape' of peptide-MHC recognition. *Nat. Immunol.* 6:171–180. doi:10.1038/ni1155

Boulter, J.M., M. Glick, P.T. Todorov, E. Baston, M. Sami, P. Rizkallah, and B.K. Jakobsen. 2003. Stable, soluble T-cell receptor molecules for crystallization and therapeutics. *Protein Eng.* 16:707–711. doi:10.1093/protein/gzg087

Brunger, A.T. 2007. Version 1.2 of the Crystallography and NMR system. *Nat. Protoc.* 2:2728–2733. doi:10.1038/nprot.2007.406

Burrows, S.R., Z. Chen, J.K. Archbold, F.E. Tynan, T. Beddoe, L. Kjer-Nielsen, J.J. Miles, R. Khanna, D.J. Moss, Y.C. Liu, et al. 2010. Hard wiring of T cell receptor specificity for the major histocompatibility complex is underpinned by TCR adaptability. *Proc. Natl. Acad. Sci. USA.* 107:10608–10613. doi:10.1073/pnas.1004926107

Cole, D.K., N.J. Pumphrey, J.M. Boulter, M. Sami, J.I. Bell, E. Gostick, D.A. Price, G.F. Gao, A.K. Sewell, and B.K. Jakobsen. 2007. Human TCR-binding affinity is governed by MHC class restriction. *J. Immunol.* 178:5727–5734.

Collaborative Computational Project, Number 4. 1994. The CCP4 suite: programs for protein crystallography. *Acta Crystallogr. D Biol. Crystallogr.* 50:760–763. doi:10.1107/S0907444994003112

Costantini, S., A. Paladino, and A.M. Facchiano. 2008. CALCOM: a software for calculating the center of mass of proteins. *Bioinformation.* 2:271–272.

Dai, S., E.S. Huseby, K. Rubtsova, J. Scott-Browne, F. Crawford, W.A. Macdonald, P. Marrack, and J.W. Kappler. 2008. Crossreactive T Cells spotlight the germline rules for alphabeta T cell-receptor interactions with MHC molecules. *Immunity.* 28:324–334. doi:10.1016/j.immuni.2008.01.008

Day, C.L., N.P. Seth, M. Lucas, H. Appel, L. Gauthier, G.M. Lauer, G.K. Robbins, Z.M. Szczepiorkowski, D.R. Casson, R.T. Chung, et al. 2003. Ex vivo analysis of human memory CD4 T cells specific for hepatitis C virus using MHC class II tetramers. *J. Clin. Invest.* 112:831–842.

Ellmerich, S., M. Mycko, K. Takacs, H. Waldner, F.N. Wahid, R.J. Boyton, R.H. King, P.A. Smith, S. Amor, A.H. Herlihy, et al. 2005. High incidence of spontaneous disease in an HLA-DR15 and TCR transgenic multiple sclerosis model. *J. Immunol.* 174:1938–1946.

Emsley, P., and K. Cowtan. 2004. Coot: model-building tools for molecular graphics. *Acta Crystallogr. D Biol. Crystallogr.* 60:2126–2132. doi:10.1107/S0907444904019158

Fairchild, P.J., R. Wildgoose, E. Atherton, S. Webb, and D.C. Wraith. 1993. An autoantigenic T cell epitope forms unstable complexes with class II MHC: a novel route for escape from tolerance induction. *Int. Immunol.* 5:1151–1158. doi:10.1093/intimm/5.9.1151

Feng, D., C.J. Bond, L.K. Ely, J. Maynard, and K.C. Garcia. 2007. Structural evidence for a germline-encoded T cell receptor–major histocompatibility complex interaction 'codon'. *Nat. Immunol.* 8:975–983. doi:10.1038/ni1502

Garboczi, D.N., P. Ghosh, U. Utz, Q.R. Fan, W.E. Biddison, and D.C. Wiley. 1996. Structure of the complex between human T-cell receptor, viral peptide and HLA-A2. *Nature*. 384:134–141. doi:10.1038/384134a0

Garcia, K.C., and E.J. Adams. 2005. How the T cell receptor sees antigen—a structural view. *Cell*. 122:333–336. doi:10.1016/j.cell.2005.07.015

Garcia, K.C., M. Degano, R.L. Stanfield, A. Brunmark, M.R. Jackson, P.A. Peterson, L. Teyton, and I.A. Wilson. 1996. An alphabeta T cell receptor structure at 2.5 A and its orientation in the TCR-MHC complex. *Science*. 274:209–219. doi:10.1126/science.274.5285.209

Garcia, K.C., M. Degano, L.R. Pease, M. Huang, P.A. Peterson, L. Teyton, and I.A. Wilson. 1998. Structural basis of plasticity in T cell receptor recognition of a self peptide-MHC antigen. *Science*. 279:1166–1172. doi:10.1126/science.279.5354.1166

Garcia, K.C., J.J. Adams, D. Feng, and L.K. Ely. 2009. The molecular basis of TCR germline bias for MHC is surprisingly simple. *Nat. Immunol.* 10:143–147. doi:10.1038/ni.f.219

Goverman, J., A. Woods, L. Larson, L.P. Weiner, L. Hood, and D.M. Zaller. 1993. Transgenic mice that express a myelin basic protein-specific T cell receptor develop spontaneous autoimmunity. *Cell*. 72:551–560. doi:10.1016/0092-8674(93)90074-Z

Gras, S., S.R. Burrows, L. Kjer-Nielsen, C.S. Clements, Y.C. Liu, L.C. Sullivan, M.J. Bell, A.G. Brooks, A.W. Purcell, J. McCluskey, and J. Rossjohn. 2009. The shaping of T cell receptor recognition by self-tolerance. *Immunity*. 30:193–203. doi:10.1016/j.immuni.2008.11.011

Hahn, M., M.J. Nicholson, J. Pyrdol, and K.W. Wucherpfennig. 2005. Unconventional topology of self peptide-major histocompatibility complex binding by a human autoimmune T cell receptor. *Nat. Immunol.* 6:490–496. doi:10.1038/ni1187

Hare, B.J., D.F. Wyss, M.S. Osburne, P.S. Kern, E.L. Reinherz, and G. Wagner. 1999. Structure, specificity and CDR mobility of a class II restricted single-chain T-cell receptor. *Nat. Struct. Biol.* 6:574–581. doi:10.1038/9359

Harrington, C.J., A. Paez, T. Hunkapiller, V. Mannikko, T. Brabb, M. Ahearn, C. Beeson, and J. Goverman. 1998. Differential tolerance is induced in T cells recognizing distinct epitopes of myelin basic protein. *Immunity*. 8:571–580. doi:10.1016/S1074-7613(00)80562-2

He, X.L., C. Radu, J. Sidney, A. Sette, E.S. Ward, and K.C. Garcia. 2002. Structural snapshot of aberrant antigen presentation linked to autoimmunity: the immunodominant epitope of MBP complexed with I-Au. *Immunity*. 17:83–94. doi:10.1016/S1074-7613(02)00340-0

Hennecke, J., A. Carfi, and D.C. Wiley. 2000. Structure of a covalently stabilized complex of a human alphabeta T-cell receptor, influenza HA peptide and MHC class II molecule, HLA-DR1. *EMBO J.* 19:5611–5624. doi:10.1093/emboj/19.21.5611

Huseby, E.S., J. White, F. Crawford, T. Vass, D. Becker, C. Pinilla, P. Marrack, and J.W. Kappler. 2005. How the T cell repertoire becomes peptide and MHC specific. *Cell*. 122:247–260. doi:10.1038/ni1401

Huseby, E.S., F. Crawford, J. White, P. Marrack, and J.W. Kappler. 2006. Interface-disrupting amino acids establish specificity between T cell receptors and complexes of major histocompatibility complex and peptide. *Nat. Immunol.* 7:1191–1199. doi:10.1038/ni1401

Ishikura, H., N. Ishikawa, and M. Aizawa. 1987. Differential expression of HLA-class II antigens in the human thymus. Relative paucity of HLA-DQ antigens in the thymic medulla. *Transplantation*. 44:314–317. doi:10.1097/00007890-198708000-00026

Lafaille, J.J., K. Nagashima, M. Katsuki, and S. Tonegawa. 1994. High incidence of spontaneous autoimmune encephalomyelitis in immunodeficient anti-myelin basic protein T cell receptor transgenic mice. *Cell*. 78:399–408. doi:10.1016/0092-8674(94)90419-7

Laskowski, R.A., M.W. MacArthur, D.S. Moss, and J.M. Thornton. 1993. PROCHECK - a program to check the stereochemical quality of protein structures. *J. Appl. Crystallogr.* 26:283–291. doi:10.1107/S0021889892009944

Lee, B., and F.M. Richards. 1971. The interpretation of protein structures: estimation of static accessibility. *J. Mol. Biol.* 55:379–400. doi:10.1016/0022-2836(71)90324-X

Li, Y., Y. Huang, J. Lue, J.A. Quandt, R. Martin, and R.A. Mariuzza. 2005. Structure of a human autoimmune TCR bound to a myelin basic protein self-peptide and a multiple sclerosis-associated MHC class II molecule. *EMBO J.* 24:2968–2979. doi:10.1038/sj.emboj.7600771

Madsen, L.S., E.C. Andersson, L. Jansson, M. krogsgaard, C.B. Andersen, J. Engberg, J.L. Strominger, A. Svejgaard, J.P. Hjorth, R. Holmdahl, et al. 1999. A humanized model for multiple sclerosis using HLA-DR2 and a human T-cell receptor. *Nat. Genet.* 23:343–347. doi:10.1038/15525

Manning, T.C., C.J. Schlueter, T.C. Brodnicki, E.A. Parke, J.A. Speir, K.C. Garcia, L. Teyton, I.A. Wilson, and D.M. Kranz. 1998. Alanine scanning mutagenesis of an alphabeta T cell receptor: mapping the energy of antigen recognition. *Immunity*. 8:413–425. doi:10.1016/S1074-7613(00)80547-6

Marrack, P., J.P. Scott-Browne, S. Dai, L. Gapin, and J.W. Kappler. 2008. Evolutionarily conserved amino acids that control TCR-MHC interaction. *Annu. Rev. Immunol.* 26:171–203. doi:10.1146/annurev.immunol.26.021607.090421

Maynard, J., K. Petersson, D.H. Wilson, E.J. Adams, S.E. Blondelle, M.J. Boulanger, D.B. Wilson, and K.C. Garcia. 2005. Structure of an autoimmune T cell receptor complexed with class II peptide-MHC: insights into MHC bias and antigen specificity. *Immunity*. 22:81–92.

McCoy, A.J., R.W. Grosse-Kunstleve, P.D. Adams, M.D. Winn, L.C. Storoni, and R.J. Read. 2007. Phaser crystallographic software. *J. Appl. Cryst.* 40:658–674. doi:10.1107/S0021889807021206

Otwinowski, Z., and W. Minor. 1997. Processing of x-ray diffraction data collected in oscillation mode. *Methods Enzymol.* 276:307–326. doi:10.1016/S0076-6879(97)76066-X

Pearson, C.I., W. van Ewijk, and H.O. McDevitt. 1997. Induction of apoptosis and T helper 2 (Th2) responses correlates with peptide affinity for the major histocompatibility complex in self-reactive T cell receptor transgenic mice. *J. Exp. Med.* 185:583–599. doi:10.1084/jem.185.4.583

Reinherz, E.L., K. Tan, L. Tang, P. Kern, J. Liu, Y. Xiong, R.E. Hussey, A. Smolyar, B. Hare, R. Zhang, et al. 1999. The crystal structure of a T cell receptor in complex with peptide and MHC class II. *Science*. 286:1913–1921. doi:10.1126/science.286.5446.1913

Reiser, J.B., C. Darnault, A. Guimezanes, C. Grégoire, T. Mosser, A.M. Schmitt-Verhulst, J.C. Fontecilla-Camps, B. Malissen, D. Housset, and G. Mazza. 2000. Crystal structure of a T cell receptor bound to an allogeneic MHC molecule. *Nat. Immunol.* 1:291–297. doi:10.1038/79728

Roucard, C., F. Garban, N.A. Mooney, D.J. Charron, and M.L. Ericson. 1996. Conformation of human leukocyte antigen class II molecules. Evidence for superdimers and empty molecules on human antigen presenting cells. *J. Biol. Chem.* 271:13993–14000. doi:10.1074/jbc.271.24.13993

Rudolph, M.G., R.L. Stanfield, and I.A. Wilson. 2006. How TCRs bind MHCs, peptides, and coreceptors. *Annu. Rev. Immunol.* 24:419–466. doi:10.1146/annurev.immunol.23.021704.115658

Scott-Browne, J.P., J. White, J.W. Kappler, L. Gapin, and P. Marrack. 2009. Germline-encoded amino acids in the alphabeta T-cell receptor control thymic selection. *Nature*. 458:1043–1046. doi:10.1038/nature07812

Siebold, C., B.E. Hansen, J.R. Wyer, K. Harlos, R.E. Esnouf, A. Svejgaard, J.I. Bell, J.L. Strominger, E.Y. Jones, and L. Fugger. 2004. Crystal structure of HLA-DQ0602 that protects against type 1 diabetes and confers strong susceptibility to narcolepsy. *Proc. Natl. Acad. Sci. USA*. 101:1999–2004. doi:10.1073/pnas.0308458100

Sim, B.C., L. Zerva, M.I. Greene, and N.R. Gascoigne. 1996. Control of MHC restriction by TCR Valpha CDR1 and CDR2. *Science*. 273:963–966. doi:10.1126/science.273.5277.963

Smith, K.J., J. Pyrdol, L. Gauthier, D.C. Wiley, and K.W. Wucherpfennig. 1998. Crystal structure of HLA-DR2 (DRA*0101, DRB1*1501) complexed with a peptide from human myelin basic protein. *J. Exp. Med.* 188:1511–1520. doi:10.1084/jem.188.8.1511

Stanley, P. 1989. Chinese hamster ovary cell mutants with multiple glycosylation defects for production of glycoproteins with minimal carbohydrate heterogeneity. *Mol. Cell. Biol.* 9:377–383.

Sun, R., S.E. Shepherd, S.S. Geier, C.T. Thomson, J.M. Sheil, and S.G. Nathenson. 1995. Evidence that the antigen receptors of cytotoxic T lymphocytes interact with a common recognition pattern on the H-2Kb molecule. *Immunity*. 3:573–582. doi:10.1016/1074-7613(95)90128-0

Teng, M.K., A. Smolyar, A.G. Tse, J.H. Liu, J. Liu, R.E. Hussey, S.G. Nathenson, H.C. Chang, E.L. Reinherz, and J.H. Wang. 1998. Identification of a common docking topology with substantial variation among different TCR-peptide-MHC complexes. *Curr. Biol.* 8:409–412. doi:10.1016/S0960-9822(98)70160-5

Turner, S.J., P.C. Doherty, J. McCluskey, and J. Rossjohn. 2006. Structural determinants of T-cell receptor bias in immunity. *Nat. Rev. Immunol.* 6:883–894. doi:10.1038/nri1977

Tynan, F.E., S.R. Burrows, A.M. Buckle, C.S. Clements, N.A. Borg, J.J. Miles, T. Beddoe, J.C. Whisstock, M.C. Wilce, S.L. Silins, et al. 2005. T cell receptor recognition of a 'super-bulged' major histocompatibility complex class I-bound peptide. *Nat. Immunol.* 6:1114–1122. doi:10.1038/ni1257

Tynan, F.E., H.H. Reid, L. Kjer-Nielsen, J.J. Miles, M.C. Wilce, L. Kostenko, N.A. Borg, N.A. Williamson, T. Beddoe, A.W. Purcell, et al. 2007. A T cell receptor flattens a bulged antigenic peptide presented by a major histocompatibility complex class I molecule. *Nat. Immunol.* 8:268–276. doi:10.1038/ni1432

Vagin, A., and A. Teplyakov. 1997. MOLREP: an automated program for molecular replacement. *J. Appl. Crystallogr.* 30:1022–1025. doi:10.1107/S0021889897006766

Wu, L.C., D.S. Tuot, D.S. Lyons, K.C. Garcia, and M.M. Davis. 2002. Two-step binding mechanism for T-cell receptor recognition of peptide MHC. *Nature.* 418:552–556. doi:10.1038/nature00920

Wucherpfennig, K.W., and J.L. Strominger. 1995. Molecular mimicry in T cell-mediated autoimmunity: viral peptides activate human T cell clones specific for myelin basic protein. *Cell.* 80:695–705. doi:10.1016/0092-8674(95)90348-8

Wucherpfennig, K.W., A. Sette, S. Southwood, C. Oseroff, M. Matsui, J.L. Strominger, and D.A. Hafler. 1994a. Structural requirements for binding of an immunodominant myelin basic protein peptide to DR2 isotypes and for its recognition by human T cell clones. *J. Exp. Med.* 179:279–290. doi:10.1084/jem.179.1.279

Wucherpfennig, K.W., J. Zhang, C. Witek, M. Matsui, Y. Modabber, K. Ota, and D.A. Hafler. 1994b. Clonal expansion and persistence of human T cells specific for an immunodominant myelin basic protein peptide. *J. Immunol.* 152:5581–5592.

Wucherpfennig, K.W., M.J. Call, L. Deng, and R. Mariuzza. 2009. Structural alterations in peptide-MHC recognition by self-reactive T cell receptors. *Curr. Opin. Immunol.* 21:590–595. doi:10.1016/j.coi.2009.07.008